International Journal of Advanced Trends in Engineering and Management
(ISSN 2583-7052)

Vol. IV, No. 11, pp. 21-31, November

An Integrated Approach for Pneumonia Diagnosis using Inception V_3 Classifier

Karthika K[1*]

[1]Associate Professor, Department of Computer Science and Engineering, Sri Sairam College of Engineering, Anekal, Bangalore, karthikakphd@gmail.com

[1*]Corresponding Author E-mail: karthikakphd@gmail.com

ABSTRACT: A significant number of people are susceptible to pneumonia, a potentially fatal respiratory illness, especially in places with high pollution, dense populations, unhygienic environments and inadequate medical facilities. Pericardial effusion, a condition where fluid accumulates in the chest and impairs breathing, is usually the result of pneumonia. Pneumonia ought to be diagnosed promptly and accurately in order to treated effectively and increase survival rates. Pneumonia is often manually detected by specialists, but this method is laborious and prone to human error, making it ineffective for processing a large number of images. The proposed framework encompasses four stages: image preprocessing, segmentation, feature extraction and classifier. In this study an effective image preprocessing approach, Contrast Limited Adaptive Histogram Equalization (CLAHE) is implemented for reducing the noise amplification. K −means clustering is employed for dividing the noise-free image into numerous regions. Inception V_3 is used to classify the features that were extracted misinterpretation and improve patient outcomes, while Wavelet Transform (WT) is employed to extract the best characteristics of the segmented image for precise and effective diagnosis. An efficient implementation of Python is used to assess the methodology's overall performance. The data collected indicate that the suggested classifier results with a maximum accuracy of 95.67% compared to the existing classifiers.

Keywords: Pneumonia, CLAHE, K −means clustering, Wavelet transform, Inception V_3.

1. Introduction

A serious and potentially dangerous respiratory illness, pneumonia primarily impacts susceptible groups like infants, elderly individuals, young children and those with weakened immune systems. Mycoplasma pneumonia, viral pneumonia, bacterial pneumonia and other forms of pneumonia are among the several forms of pneumonia [1]. Bacterial pneumonia is caused by bacteria or fungus, and it cause a number of symptoms, including immune system weakness, aging, disease, poor nutrition and weakness of the body. People of all ages are at risk, but people who smoke, drink, recently underwent surgery, suffer from asthma, possess a viral infection or a compromised immune system are at higher risk. Nearly one-third of all pneumonia cases are caused by several viruses, including the flu. All stage individuals are usually impacted by Mycoplasma pneumonia, additionally referred to as typical pneumonia that is caused by a bacterium [2-3].

Early detection of pneumonia and prompt administration of suitable treatment significantly decrease the possibility of a patient's condition worsening and eventually dying. In order to stop the disease from progressing to a deadly level, initial detection and maintenance are therefore crucial [4]. Computed Tomography (CT), Magnetic Resonance Imaging (MRI) and radiography (X-rays) are frequently used for radiographic assessment of the lungs for diagnosis. Chest X-ray images represent the preferable technology in diagnosis pneumonia; however, these images are somewhat not obvious and sometimes misclassified to benign abnormalities or other diseases by the expert radiologists, which lead to giving the wrong medicine to the patients and subsequently deteriorating the patient's situation [5]. In order to properly identify pneumonia disease in its early stages and achieve the most effective results, the image is processed through four distinct stages like image preprocessing, segmentation, feature abstraction and organisation. The input image is first subjected to the denoising process, which eliminates undesired inherent noises to improve image quality. As a result, a variety of filters are used in this process to filter the input image; initially, the linear filter is recommended because it effectively reduces the noise content in the images. Nonetheless, the drawback of the filter is that it blurs the image's contrast and edges, which limits its utility [6]. Hence, the mean and median filters are preferred in order to counteract the drawbacks of linear filters. These filters are sufficiently effective at eliminating noise from images while maintaining edge information, but the application is limited due to their low accuracy. Thus, the current study suggests employing a CLAHE filter to achieve the most effective results from image preprocessing [7].

After the completion of noise reduction, the second stage known as segmentation, divides the noises into several portions in order to improve the ease of disease diagnosis with the highest level of accuracy. Several methods are used to segment the images, although numerous research studies prefer the Otsu technique since it produces the best results with the highest precision. However, it is unsuitable for many applications due to its instability to determine the global threshold under specific circumstances. This study introduces segmentation using k −means clustering to optimally limit all these drawbacks [8]. It offers advantages such as high dependability and quick convergence throughout the segmentation process. The third step involves extracting the most effective features from the segmented images utilizing appropriate methods to improve the precision of identifying the presence of disease across a larger range. The use of the Gray Level Co-occurrence Matrix (GLCM) is thought to be the best method among various algorithms in the early stages since it effectively extract the best features without removing the image's edge information, but its wide range of applications is limited by its difficulty in requiring less accuracy. The Wavelet Transform strategy is used in this work to effectively overcome the drawbacks of these methods throughout the feature extraction process [9].

The extracted image is subsequently organized to efficiently classify the types and stages of pneumonia disease. Initially, various classifiers, including Decision Tree (DT), Support Vector Machine (SVM) and Random Forest (RF), was used to classify the images since their classification accuracy proved to be best, however their computational complexity became a barrier to their use. Thus, the Deep Neural Network (DNN) classifier is presented for classifying the image without any complications but the unknown duration becomes a disadvantage of consuming this classifier. To overcome these issues the present study employs Inception V_3 classifier in the grouping process for attaining ideal outcomes without any obstacles [10].

The main contribution of this research includes:

- To enhance the resolution of the input image CLAHE approach is implemented in image preprocessing for reducing the unwanted noise amplification.
- To effectively segment the image K −means clustering is introduced to improve the reliability and fast convergence.

- To extract prominent features, wavelet transform in feature extraction is employed to discriminate between healthy and diseased lungs.
- To accurately detect pneumonia disease, Inception V_3 classifier is applied.

2. Literature Survey

Bing *et al* (2025) have established a Machine Learning (ML) based models for organ damage risk prediction and differential diagnosis for Severe Mycoplasma Pneumonia (SMP) in children. The objective is to create and evaluate ML for the early detection and risk assessment of liver damage in children with severe mycoplasma pneumonia. The models utilize accessible laboratory indicators and ML algorithms to differentiate SMP from other respiratory illness and predict the risk of liver damage. However, these include limited data, the need for validation in larger populations and the potential for overfitting.

Usman *et al* (2025) have proposed a ML and chest X-rays for the identification of pneumonia disease. It employs Artificial Intelligence (AI) techniques to analyze medical images and identify signs of pneumonia automatically. This approach aims to assist radiologists, improve diagnostic speed, accuracy and potentially reduce the workload on medical professionals. Nevertheless, the reliance on X-rays are problematic due to variations in image quality and subjective interpretations, potentially leading to delayed or inaccurate diagnosis.

Deng *et al* (2025) have implemented a Deep Learning (DL) and radiomics to automatically identify and distinguish among bacterial pneumonia and pulmonary contusion. This approach automatically differentiate between pulmonary contusion and bacterial pneumonia on chest CT- scans. Based on radiomics features, a massive amount of numerical structures from remedial images, potentially revealing subtle patterns not visible to the naked eye. Nonetheless, it need high quality datasets for training and the complexity of interpreting the extracted features. Additionally, it makes difficult to understand their decision-making process.

Asnake *et al* (2024) have developed a DL-based pneumonia detection and classification system based on X-ray images. DL works well for classifying and detecting pneumonia from chest x-ray images. These models analyze the images to identify patterns indicative of pneumonia, achieving high accuracy and aiding in faster, more accurate diagnosis. Though, it includes various drawbacks such as the potential for bias in training data and challenges in generalizing to different image techniques and patient populations. They still miss subtle signs of pneumonia or misinterpret other lung conditions, potentially leading to unnecessary treatment.

Alshanketi *et al* (2024) have established a pneumonia detection from chest X-ray images using DL and transfer learning (TL) for imbalanced datasets. DL and TL are effectively used for pneumonia detection from chest X-ray images, especially when dealing with imbalanced datasets.TL allows pre-trained models to be adapted to the specific task of pneumonia detection, leveraging their learned features and reducing the need for extensive training data. However, it requires a careful evaluation of model performance in the presence of imbalanced data and difficulty in explaining model decisions.

3. Proposed System

This paper presents an extensive description regarding the implementation of Inception V_3 based image preprocessing approach which is used to diagnose pneumonia at an early stage. This approach is capable of accurately predicting the disease, which helps to achieve the eventual goal of recognising the incidence of lung disease without any complications. The performance efficiency of this method is really good since it helps to provide necessary medical interventions promptly by efficiently classifying the image for predicting the pneumonia sickness. Figure 1 displays the block diagram for the suggested method.

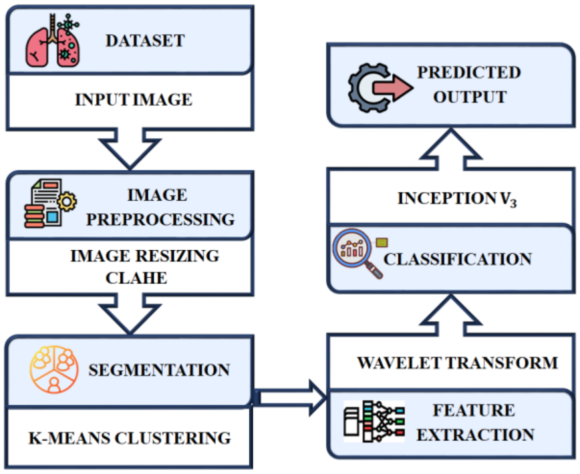

Figure 1: *Block diagram of the proposed approach*

After the completion of the primary data accumulating task, the input images is fed into the first stage, known as preprocessing where CLAHE effectively eliminates all inevitable or undesirable noises from the images, enhancing them in the best possible way. To increase the accuracy of disease diagnosis, the denoised image is then divided into several portions in the second stage using k-means clustering. Following the segmentation process, the WT technique is used to effectively extract the features from the segmented images in the subsequent step. This greatly lessens the difficulties in determining whether pneumonia disease is present. The final step involves effectively classifying the segmented features using Inception V_3 classifier, which aids in the most efficient diagnosis of illness types and stages. As a result, the proposed methodology is highly suitable for use in the process of detecting pneumonia.

4. Proposed System Modelling

To effectively emphasize the performance metrics of this approach, an extensive description and modelling processes of the four stages involved in the image processing approach are included below.

4.1 Image Preprocessing

Low contrast and noise are common problems with chest x-ray images, which conceal crucial diagnostic characteristics for classifying pneumonia. By splitting an image into tiles and using histogram equalization with a contrast limit to stop noise amplification, the CLAHE approach improves local contrast. The predefined parameters used in standard CLAHE potentially over emphasize homogeneous areas, such as soft tissues. In order to maximize improvement for chest x-rays and produce improved image quality, the suggested CLAHE algorithm presents adaptive tile scaling, variance directed histogram clipping, and entropy subjective rearrangement. Figure 2 shows the flow diagram for data preprocessing with CLAHE.

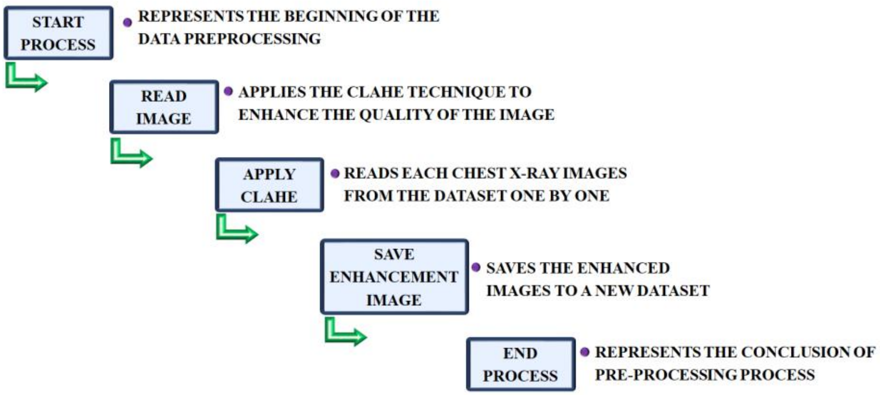

Figure 2: *Flow diagram for data preprocessing using CLAHE*

In image processing systems, histogram equalization is frequently employed to improve contrast, especially in images with closely spaced intensity values. This technique makes low contrast areas more visible while increasing overall contrast. Block Size (BS) and Clipping Limit (CL) are the two crucial parameters of the CLAHE approach, are essential for improved image quality. Indeed, the image gets brighter when the CL is constrained. This is because the original image produced a flatter histogram due to its very low intensity and greater CL value. The CL formula is displayed below.

$$CL_{base} = 0.03 + \alpha * \frac{\sigma_{hist}}{\sigma_{hist,max}} \quad (1)$$

Increasing the CL causes the image's dynamic range to increase, which raises the contrast of the image. The improved output image is thus obtained and the filtered image is subsequently supplied to the segmentation stage, which is the second method.

4.2 Segmentation

After image preparation, all image quality and resolution are standardized. Images are subjected to image segmentation in order to extract features or other pertinent information for image classification. An image is capable of being divided into k clusters using the k −means based clustering algorithm, which is an unsupervised pixel segmentation technique. Each cluster contains its own cluster center vector. Each pixel vector's Euclidean distance to the cluster center is determined. Consider, there are $x * y$ pixels in the image. Based on the closest jth cluster center, the k −means clustering enables the individual division of all $x * y$ pixels. The following are instances of ways that k −means clustering is used for image segmentation.

- First, obtain the image's minimum and highest pixel levels $\left(min_{p(x,y)}, max_{p(x,y)}\right)$. After that, determine c_j, the initial cluster vector.

$$c_j = min_{p(x,y)} + (2j+1)\left(\frac{max_{p(x,y)} - min_{p(x,y)}}{2n_c}\right) \quad (2)$$

- Afterwards, calculate the c_j and the Euclidean distance, d for each pixel vector.

$$d = \| p(x,y) - c_j \| \quad (3)$$

- Based on the d, allocate each pixel point to the closest center vector, c_j.
- Next, use the concept of means formula to compute the new cluster center vector, $c_{j_{new}}$.

$$c_{j_{new}} = \frac{1}{n_j} \sum_{y \in c_j} \sum_{x \in c_j} p(x,y) \quad (4)$$

- Repeat the steps 2 to 4 until $c_{j_{new}}$ maintains the same value as the prior outcome. Figure 3 displays a flowchart for k −means clustering-based image segmentation.

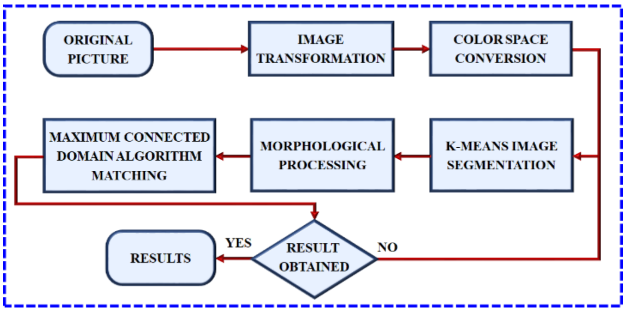

Figure 3: *Flowchart for image segmentation*

Since it helps to maximize the system's overall reliability in diagnosing pneumonia, the consequence of this k −means clustering is exceptionally high in terms of separating the images in an ideal method. The segmented images are supplied to the following step for the extraction of the best features when the segmentation process is finished.

4.3 Feature Extraction

The segmented image's feature extraction process is considered a crucial step in the overall operation of this approach as it involves effectively choosing and retaining the relevant diagnostic information from the original image to increase the probability of disease detection across a larger range. In this paper Wavelet Transform (WT) are implemented in feature extraction process. WT is a powerful tool in medical image analysis, particularly for pneumonia detection, where it helps extract key features from chest X-rays. By decomposing images into different frequency components, wavelet transform captures both spatial and frequency information, which can highlight subtle changes indicative of pneumonia.

The two main categories of WT are Discrete Wavelet Transform (DWT) and Continuous Wavelet Transform (CWT). DWT is applied on each feature to obtain a set of coefficients for each feature. Mathematically for feature i and j are as follows,

$$Coeff, s_i = [A_{i,1}, D_{i,1}, A_{i,2}, D_{i,2}, \ldots . A_{i,j}, D_{i,j}] \quad (5)$$

For all features, the transformed dataset $X_{transformed}$ is,

$$X_{transformed} = [coeffs_1 \parallel coeffs_2 \parallel .. \parallel coeffs_m] \quad (6)$$

Where, CWT allows for time-frequency analysis, which is useful for identifying subtle patterns and characteristics in these images are missed by other methods. CWT is particularly effective at identifying and localizing transient events, sudden changes, and discontinuities within a signal. This ability makes it valuable in applications like fault diagnosis, where subtle changes in signal patterns can indicate impending issues.

The WT-based method performs an excellent task of extracting the best features, which are subsequently passed to the last step for the best possible image classification.

4.4 Classification

In the final phase, the extracted chest x-ray image is classified using Inception V_3 classifier, which is regarded as a commonly utilized method in the classification process since it produce the best results with the highest accuracy and fastest convergence. The Inception V_3 is a CNN architecture that enhances accuracy and efficiency for applications involving object detection and image categorization. Inception V_3 adds factorized convolutions for efficiency in computation, mathematically represented in equation 7 as two consecutive convolutions.

$$Y^{(l)} = f\left(W_{1*k}^{(l)} * \left(f\left(W_{k*1}^{(l)} * X^{(i-1)}\right)\right)\right) \quad (7)$$

Where, $Y^{(l)}$ is the final output after factorized convolutions, W_{1*K} and W_{K*1} are convolutional kernels applied subsequently, f remains the activation function. Figure 4 displays pneumonia detection using Inception V_3 classifier.

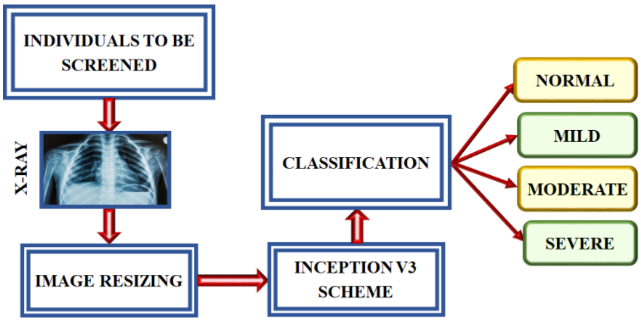

Figure 4: *Pneumonia detection using Inception V_3 classifier*

The usage of inception modules, which carry out parallel convolutions at various spatial scales and concatenate their outputs, represents a few of Inception V_3's primary characteristics. Performance is enhanced by this design, which enables the system to capture a large number of features at various levels of abstraction. To further improve speed and lessen overfitting, Inception V_3 uses strategies including aggressive regularization, factorized convolutions and batch normalization. On benchmark datasets like picture net, where it earned the best result in image classification contests, Inception V_3 is renowned for its excellent accuracy. Additionally, it continuous to be extensively employed in a number of applications, including object identification, image segmentation and image recognition. Even though it performs smoothly Inception V_3 is computationally demanding, needing a large number of processing power for both training and interference. As a result, the output generated was confirmed that Inception V_3 is highly significant in the classification process for diagnosing pneumonia.

5. Result and Discussion

This work provides a notable explanation of the manner in which the Inception V_3 classifier is implemented in order to accurately diagnose pneumonia disease in utilizing wavelet transform-based feature extraction. The results produced are then executed in Python, which is utilized to optimally validate the present study.

Table 1: *Comparative analysis of train images and test images*

Label	Train images	Test images
Normal	1248	260
Pneumonia	3384	758
Total	4632	1018

This table shows the number of chest x-ray images used to train and test a model for classifying between normal and pneumonia cases. During training, there are 1248 images of normal lungs and 3384 images display pneumonia, making a total of 4632 train images. For testing, there are 260 normal lungs and 758 pneumonia images, creating a total of 1018 test images.

Graph 1: *Comparison of train and test image distribution*

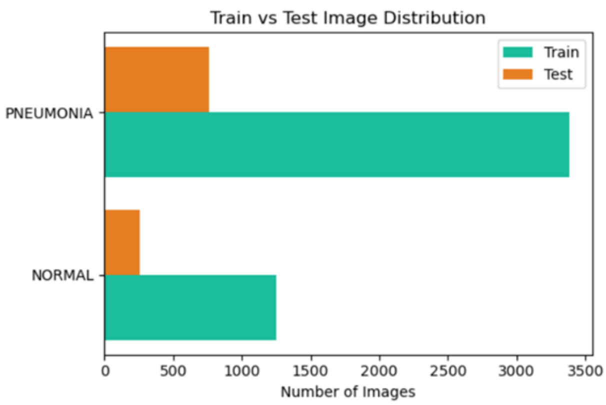

The bar graph shows the distribution of training and testing images for two classes, pneumonia and normal, with a significantly higher number of training images for both the classes compared to the test images. Specially, the pneumonia class has the largest number of training images, totally over 3000, while its corresponding test set contains fewer than 1000 images. Similarly, the normal class has approximately 1300 training images and smaller set of 200-300 test images.

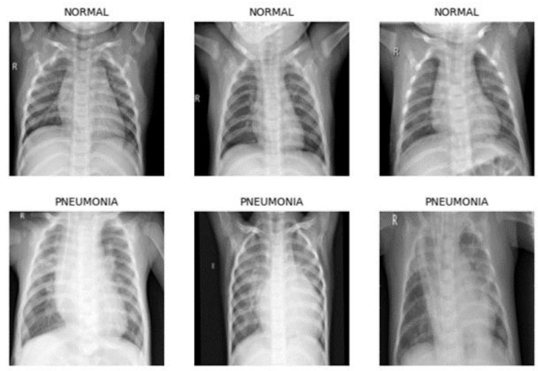

Figure 5: *Random train images*

The diagram displays a set of six chest x-ray train images, showcasing samples from two categories such as normal and pneumonia. The top row contains three x-rays labeled as normal, which shows clear lungs with no visible signs of infection or fluid accumulation. In contrast, the bottom row contains three x-rays labeled as pneumonia, where the lungs display inflammation commonly associated with pneumonia.

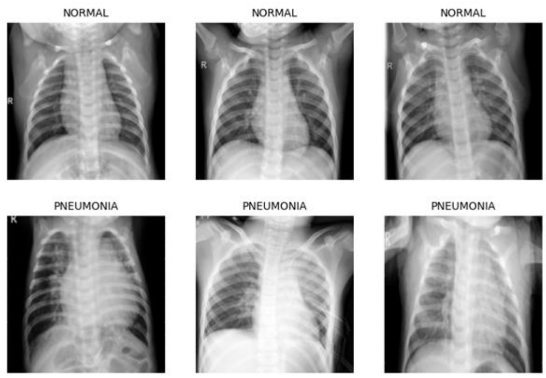

Figure 6: *Random test images*

The diagram presents a grid of six chest x-ray images, illustrate the visual differences between healthy lungs and those affected by pneumonia. The top row displays the normal x-ray images, showing perfect lungs without any infection. The bottom row displays pneumonia affected lungs that appear cloudier than the normal images.

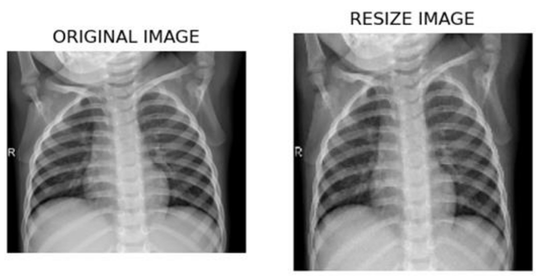

Figure 7: *Original and Resize image*

The diagram shows the comparison of original and resize image. This comparison illustrates the effect of image resizing on the shape and appearance of radiographic images. The image on the left labelled as original image and the image on the right side is labelled as resize image, where the chest cavity look elongated.

Figure 8: *Gray, CLAHE filtered and K- means segmented image*

The diagram displays a sequence of chest x-ray images, consisting of Gray image, CLAHE filtered image and K −means segmented image. The first image shows a typical radiographic details such as ribs and lung structures. The second image shows the result of applying CLAHE which enhances the ribs and vertebrae more distinct and visible. The third image presents the output of applying k −means clustering, a ML based segmentation technique. The sequence highlights how preprocessing and segmentation enhance feature extraction in medical imaging.

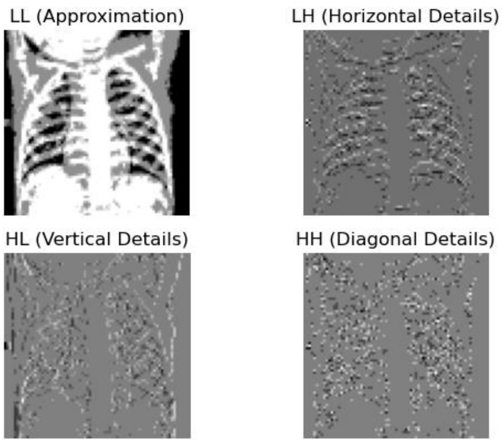

Figure 9: *Discrete Wavelet Transform of chest x-ray images*

The figure shows the DWT of chest x-ray images, which reveals different type of image details. The top image is labelled as LL (Approximations) contains low frequency, which resembles the compressed version of the original. The other three images such as LH (Horizontal details), HL (Vertical details), HH (Diagonal details) contains high frequency. These images enables better feature extraction and noise reduction.

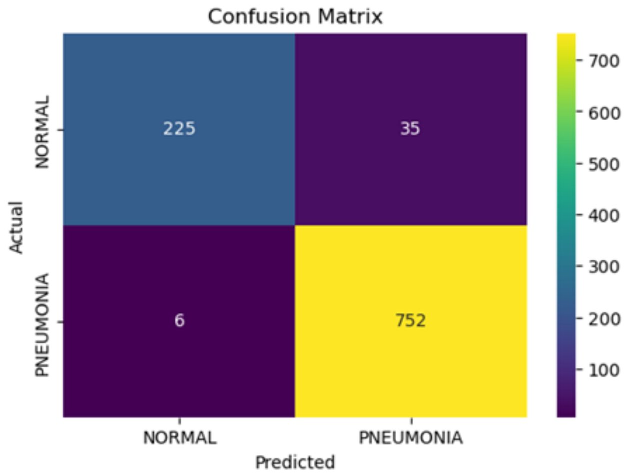

Figure 10: *Confusion matrix*

The illustration is a confusion matrix that shows the classification model in diagnosing normal and pneumonia cases. There are four quadrants in the matrix, where 225 normal cases were accurately predicted as normal, while 35 normal cases were mistakenly forecasted as pneumonia. 6 pneumonia instances were mislabelled as normal, while 752 pneumonia cases were correctly diagnosed.

Graph 2: *Receiver Operating Characteristic (ROC) curve*

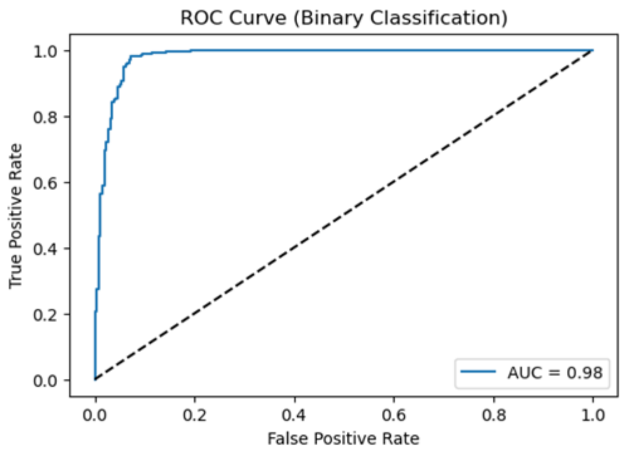

The graph illustrates the ROC curve for a binary classification model, which evaluates the trade-off between true positive rate and false positive rate across various threshold values. The ROC curve in the image rises sharply towards the top, indicating a high performance classifier and maintain a constant state of 1.0 amongst two classes.

Table 2: *Comparative analysis of various existing classifiers*

Methods	Accuracy	Precision	Recall	FI-score
SVM [16]	85%	84.2%	86%	82.6%
RF [17]	89%	86%	90%	84%
XG BOOST [18]	90.8%	92.6%	92.3%	92.4%
PROPOSED	95.97%	96%	96%	96%

The comparative analysis is carried out between various existing classifiers and proposed classifier in terms of accuracy, precision, recall and FI-score, which is remarkably listed in Table 2.

Graph 3: *Comparison of various classifiers*

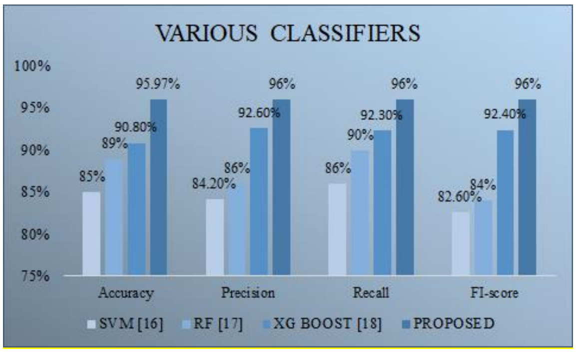

Graph 1 clearly shows the results of the comparison of different existing classifiers with regard to the performance indicators. With an accuracy of 95.67%, precision of 96%, recall of 96% and FI-score of 96%, the suggested Inception V_3 classifier outperforms the other classifiers currently in use.

6. Conclusion

The current study examines the involvement of image processing technique in the diagnosis of pneumonia disease. Through the assistance of suitable techniques, it illustrates that the chest x-ray images are processed effectively through four stages. The CLAHE filter effectively removes undesired noise from the input images, while k −means clustering successfully divides the denoised images into several sections to greatly increase the detection accuracy without any disruptions. The best features in the segmented images are optimally retrieved with the help of a WT-based technique, and the features are ultimately classified in the last stage with the use of an Inception V_3 classifier, which further helps to optimize the overall performance. Python is used to validate the complete working system, and the results shows the suggested classifier outperforms other classifiers with an ideal accuracy of 95.67%.

Reference

1. Rouba Sayegh; Li Tang; Ki Wook Yun; Zhaohui Xu; Sarah A. Marzec; Osama El-Assal; Amy L. Leber et al. Year: 2025, “Nasal mucosal cytokines as potential biomarkers for assessing Disease Severity and Class of Pathogen in Children with Community-Acquired Pneumonia”, The Journal of Infectious Diseases, Vol: 231, No: 4, pp. 1031-1040.

2. Neeta Rana; Hitesh Marwaha; Year: 2025, “Pneumonia detection from X-ray images using federated learning–an unsupervised learning approach”, Measurement: Sensors, No: 37, pp. 101410.

3. Jonathan D. Dear; Sean E. Hulsebosch; Lynelle R. Johnson; Year: 2024, “Recognition and diagnosis of underlying disease processes in bacterial pneumonia”, Animals, Vol: 14, No: 11 1601.

4. Jerald Prasath; S. Prabu; V. Valli Mayil; Sumit Saini, Year: 2025, “Optimized double transformer residual super-resolution network-based X-ray images for classification of pneumonia identification”, Knowledge-Based Systems, No: 311, pp. 113037.

5. M. Prema Kumar; Raju Porika; Rajitha Tungani; K. Sabarigirivason; B. Gunasundari; S. Saranya, Year: 2025, “Optimized Pediatric Pneumonia Detection Using Dimensionality Reduction, Class Balancing and

Transfer Learning", In 2025 6th International Conference on Recent Advances in Information Technology (RAIT), pp. 1-6.

6. Jennie Gratia Franklin, K. N. Sengamali, P. Divya, P. Prakash, P. Kasthuri, Year: 2024, "A Deep Learning Approach to Pneumonia Prediction through X-Ray Image Analysis", In International Conference on Computer Vision and Image Processing, pp. 295-307. Cham: Springer Nature Switzerland.

7. N. Shilpa; W. Ayeesha Banu; Prakash B. Metre, Year: 2024, "Revolutionizing Pneumonia Diagnosis: AI-Driven Deep Learning Framework for Automated Detection from Chest X-Rays", IEEE Access.

8. Maie Aboghazalah; Passent M. El Kafrawy; Hanaa Torkey; Ayman El-sayed, Year: 2022, "Using X-ray Image Processing Techniques to Improve Pneumonia Diagnosis based on Machine Learning Algorithms", Menoufia Journal of Electronic Engineering Research, Vol: 31, No: 1, pp. 47-54.

9. Anuj Kumar Singh; Sandeep Kumar; Sadhana Singh; Medhavi Bhardwaj, Year: 2024, "Pneumonia segmentation for infection detection using image processing technique", In Artificial Intelligence and Information Technologies, pp. 148-155. CRC Press.

10. Gisella Luisa Elena Maquen-Niño; Jhojan Genaro Nuñez-Fernandez; Fany Yesica Taquila-Calderon; Ivan Adrianzén-Olano; Percy De-La-Cruz-VdV; Gilberto Carrión-Barco, Year: 2024, "Classification Model Using Transfer Learning for the Detection of Pneumonia in Chest X-Ray Images", International Journal of Online & Biomedical Engineering, Vol: 20, No: 5.

11. Bing He; Xuewen Li; Rongrong Dong; Han Yao; Qi Zhou; Changyan Xu; Chengming Shang et al. Year: 2025, "Development of machine learning-based differential diagnosis model and risk prediction model of organ damage for severe Mycoplasma pneumonia in children", Scientific Reports, Vol: 15, No: 1, pp. 9431.

12. Cathryn Usman; Saeed Ur Rehman; Anwar Ali; Adil Mehmood Khan; Baseer Ahmad, Year: 2025, "Pneumonia Disease Detection Using Chest X-Rays and Machine Learning", Algorithms, Vol: 18, No: 2, pp. 82.

13. Tie Deng; Junbang Feng; Xingyan Le; Yuwei Xia; Feng Shi; Fei Yu; Yiqiang Zhan; Xinghua Liu; Chuanming Li, Year: 2025, "Automatic recognition and differentiation of pulmonary contusion and bacterial pneumonia based on deep learning and radiomics", BMC Medical Imaging, Vol: 25, No: 1, pp. 234.

14. Nigus Wereta Asnake; Ayodeji Olalekan Salau; Aleka Melese Ayalew, Year: 2024, "X-ray image-based pneumonia detection and classification using deep learning", Multimedia Tools and Applications, Vol: 83, No: 21, pp. 60789-60807.

15. Faisal Alshanketi; Abdulrahman Alharbi; Mathew Kuruvilla; Vahid Mahzoon; Shams Tabrez Siddiqui; Nadim Rana; Ali Tahir, Year: 2024, "Pneumonia detection from chest X-Ray images using deep learning and transfer learning for imbalanced datasets", Journal of Imaging Informatics in Medicine, pp. 1-20.

16. M. Mardianto; Alfredi Yoani; Steven Soewignjo; I. K. P. A. Putra; Deshinta Arrova Dewi. Year: 2024, "Classification of Pneumonia from Chest X-ray images using Support Vector Machine and Convolutional Neural Network", International Journal of Advanced Computer Science & Applications, Vol: 15, No: 6.

17. Mamta Patel; Mehul Shah, "Deep ensemble learning model for diagnosis of lung diseases from Chest X-Ray images. Year: 2024, "Deep ensemble learning model for diagnosis of lung diseases from Chest X-Ray images", Indian journal of science and technology, Vol: 17, No: 8, pp. 702-712.

18. Mohammed El-Ghandour; Marwa Ismael Obayya, Year: 2025, "Pneumonia detection in chest x-ray

images using an optimized ensemble with XGBoost classifier", Multimedia Tools and Applications, Vol: 84, No: 9, pp. 5491-5521.